Effects of Anthropogenic Pollutants on Biogenic Secondary Organic Aerosol Formation in the Atmosphere of Mt. Hua, China

Can Wu[1,2], Yubao Cheng[1], Yuwei Sun[1], Huijun Zhang[1], Si Zhang[1], Cong Cao[3♣],
Jianjun Li[3], Gehui Wang[1,2*]

[1]Key Lab of Geographic Information Science of the Ministry of Education, School of
  Geographic Sciences, East China Normal University, Shanghai 210062, China
[2] Institute of Eco-Chongming, 3663 North Zhongshan Road, Shanghai 200062, China
[3]State Key Laboratory of Loess and Quaternary Geology, Institute of Earth
  Environment, Chinese Academy of Sciences, Xi'an 710061, China
♣Now at Department of Chemistry, Hong Kong University of Science & Technology

*Corresponding author. Por. Gehui Wang,
Mailing address: School of Geographic Sciences, East China Normal University,
  Shanghai 210062, China
E-mail address: ghwang@geo.ecnu.edu.cn, or wanggh@ieecas.cn (Gehui Wang)

Abstract: Anthropogenic effects on biogenic secondary organic aerosol (BSOA) formation in the upper boundary layer are still not fully understood. Here, a synchronized 4-hourly monitoring of three typical BSOA tracers from isoprene, monoterpenes, β-caryophyllene and other particulate pollutants was conducted at the mountain foot (MF, 400 m a.s.l.) and mountainside (MS, 1120 m a.s.l.) of Mt. Hua, China, to investigate the chemical evolution of BSOA in air mass lifting. Our findings revealed that BSOA was the predominant source of organic matter (OM) at MS site, with an average fraction of ~43% being ~7-fold of that at MF site. As the prevalent BSOA tracer, the isoprene-derived SOA tracers ($BSOA_I$) maintained comparable level at MF site (183 ± 81 ng/m^3) and MS site (197 ± 127 ng/m^3), yet exhibited an inverse diurnal pattern between both sites. And the $BSOA_I$ fraction in OM aloft moderately decreased during the daytime, and correlated positively with 2-methyltetrols/2-methylglyceric acid ratio but negatively with NOx transported from ground level, indicating that anthropogenic NOx would significantly affect the daytime BSOA formation aloft by inhibiting the $HO_2\cdot$-pathway products. Additionally, the further formation of sulfate in lifting air mass would significantly enhance aerosol water content aloft, which suppressed the reactive uptake of isoprene epoxydiol and ultimately diminished the $BSOA_I$ yields during the daytime. These findings provide more insight into the intricate anthropogenic−biogenic interactions affecting BSOA formation in the upper boundary layer atmosphere.

Keywords: Biogenic Secondary Organic Aerosol; Isoprene; Anthropogenic pollutants; Vertical distribution

1. Introduction

Volatile organic compounds (VOCs) play a crucial role in atmospheric chemistry (Mcfiggans et al., 2019; Coggon et al., 2021), exerting profound influences on the atmospheric oxidizing capacity, tropospheric ozone burden and regional climate (Mellouki et al., 2015; Wu et al., 2020). Among the diverse VOCs, biogenic VOCs (BVOCs) primarily emitted by terrestrial vegetation predominate the global VOC flux at 1 Pg/yr (Guenther et al., 2012), exceeding anthropogenic sources by an order of magnitude. The high reactivity of dominant BVOCs (particularly, isoprene, monoterpene, and sesquiterpenes) towards O_3, OH· and NO_3· would drive rapid formation of secondary organic aerosol (SOA) (Zhang et al., 2018a; Ng et al., 2017). Consequently, these biogenically-derived SOA (BSOA) would represent a prominent contribution to global SOA budget (Kelly et al., 2018; Hodzic et al., 2016), although the models remain highly uncertain in BSOA prediction owning to the complexity of physicochemical processes involved (Hallquist et al., 2009). Given the significant climate interactions and public health implications of BSOA (Scott et al., 2014; Shrivastava et al., 2017), advancing the understanding of BSOA, including its precursors, formation processes, is urgently needed.

Over the past two decades, mounting evidence indicate that anthropogenic pollutants (e.g., SO_2, NOx) critically regulate the BSOA formation through altering oxidation pathways and gas-to-particle partitioning processes (Xu et al., 2015; Zheng et al., 2023; Xu et al., 2016). For example, sulfate, acting as an effective nucleophile, greatly promotes ring-opening reactions of isoprene epoxydiols (IEPOX) and

subsequent SOA formation, particularly organosulfates and corresponding oligomers (Cooke et al., 2024a; Xu et al., 2015); These products contribute significantly to IEPOX-driven SOA and can alter aerosol physicochemical properties (e.g., phase state, viscosity and morphology) (Lei et al., 2022; Riva et al., 2019), thereby kinetically mediating the reactive uptake of IEPOX, as well as the following SOA yield and evolution (Drozd et al., 2013; Zhang et al., 2018b; Armstrong et al., 2022). Furthermore, a recent laboratory study demonstrates that sulfate/bisulfate equilibrium also plays a critical role in BSOA formation, especially under highly acidic conditions (Cooke et al., 2024b). NOx as an important driver for BSOA formation could alter the fate of organo-peroxy radicals ($RO_2\cdot$), and subsequently affect the yield and chemical composition of BVOC-oxidized products by changing oxidation pathways (Lin et al., 2013; Pye et al., 2010). Specifically, $RO_2\cdot+HO_2\cdot$ reactions under low NOx conditions would predominantly yield low-volatility hydroperoxide species; Conversely, the reaction of NO with $RO_2\cdot$ in the high NOx regime will produce organonitrates and alkoxy radicals ($RO\cdot$) that can fragment into more volatile products. Whereas, the impact of NOx on BSOA yield is nonlinear as explored by laboratory studies (Xu et al., 2014; Kroll et al., 2006). Additionally, the abundant O_3 could also significantly promote BSOA formation via enhancing BVOCs ozonolysis. Therefore, the changes of anthropogenic emissions would potentially perturb the BSOA formation. As modeling studies demonstrated, anthropogenic emission controls substantially decreased the BSOA formation in the United States during 1990-2012 (Ridley et al., 2018), and ~ a further 35% of isoprene-derived SOA (SOA_I) would be reduced in

2025 if ongoing the similar emission regulations (Marais et al., 2016). The parallel effects also emerged in China, where the effective control on SO_2 emissions drove a significant decline of SOA_I at $-8.0\%/yr$ over 2007−2015, even being two-fold that of SO_4^{2-} (Dong et al., 2022).

Numerous studies have comprehensively characterized the surface BSOA, yet the vertical distribution of BSOA remains insufficiently understood, which is a critical driver of uncertainties in the global climate models (Nazarenko et al., 2017; Hodnebrog et al., 2014). The mountain-based observations revealed that BSOA constitutes a substantial fraction (30–60%) of aerosols in the free troposphere (Fu et al., 2014; Ren et al., 2019; Yi et al., 2021); And these elevated BSOA are significantly influenced by the valley breeze that could transport the surface pollutants to the upper boundary layer, indicating the potential effects of surface pollutant emissions on BSOA formation aloft. In addition, airborne pollutants likely undergo aging in the vertical transport process (Wu et al., 2022), causing increasingly complex compositions and changes in oxidizing capacity and aerosol properties compared with that at ground level. Consequently, more observational studies are necessary to obtain an improved understanding of the anthropogenic−biogenic interactions driving BSOA formation aloft.

Guanzhong Basin of inland China is a typical semiarid region in East Asia, suffering serious particle pollution due to the large anthropogenic emissions (Wang et al., 2016). In our previous studies (Li et al., 2013; Wang et al., 2012), the molecular distribution, evolutionary mechanism and sources of BSOA have been investigated;

Whereas the anthropogenic emissions experienced dramatic changes recently in this region (Zhang et al., 2019a), thereby, the primary factors currently driving the BSOA formation are probably distinct from those that prevailed previously. To elucidate the formation mechanism of biogenic SOA aloft in this region, synchronous observations were conducted on the mountainside and the mountain foot of Mt. Hua, which adjoins the Guanzhong basin. In this study, we firstly investigate chemical molecular compositions and diurnal variation of the of BSOA over Mt. Hua, then explored the impacts of anthropogenic pollutants on BSOA formation during the vertical transport, and finally quantified its source contributions.

2 Experiment

2.1 Sample collection

From 27 August to 17 September 2016, aerosol sampling with a 4-hr interval were synchronously conducted at two locations in Mt. Hua region, employing the high-volume air samplers with a flow rate of 1.13 m^3/min. One sampling site (34°32′N, 110°5′E, 400 m a.s.l; MF) is situated at the mountain foot of Mt. Hua, enveloped by several traffic arteries, residential and commercial buildings. Another site is located on mountainside (34°29′N, 110°3′E, 1120 m a.s.l; MS), approximately 8 km away from MF site in horizontal distance; This site is adjacent to one of the larger valleys of Mt. Hua, characterized by precipitous terrain and less anthropogenic activities. The surface-level pollutants can be transported to here by the prevailing valley breeze, which has been validated by the organic tracers and meteorological field simulated by WRF-Chem model in our previous studies (Wu et al., 2022; Wu et al., 2024). All the

aerosol samples were collected on pre-combusted (450 °C for 6 hr) quartz filters (Whatman 1851-865), which has a retention efficiency of >99.995% for DOP particles at 0.3 μm; After collection, the filter samples would be stored in a freezer (< −18 °C) prior to chemical analysis.

Additionally, the hourly concentration of the pollutants, including $PM_{2.5}$, O_3, NO_2, were also monitored at MS site by corresponding online equipment; While, those data for MF site were mainly acquired through Weinan Ecological Environment Bureau (http://sthjj.weinan.gov.cn/, last access: 8 July 2021). All meteorological data were downloaded from the Shaanxi Meteorological Bureau website (http://sn.cma.gov.cn/, last access:8 July 2021). The comprehensive details regarding the sampling sites and instrumentation were delineated in our previous studies (Wu et al., 2022; Wu et al., 2024).

2.2 Chemical analysis

The details of organic matter extraction, derivatization, and gas chromatography/mass spectrometry (GC/MS) analyses can be referred to elsewhere (Wang and Kawamura, 2005). Briefly, for the analytical procedure of organic tracers in the aerosol, one-quarter of $PM_{2.5}$ sample was cut into pieces and then ultrasonically extracted with a mixture of dichloromethane and methanol (2: 1, v/v) three times (each for 15 min). The extracts were filtered through a pasteur pipette plugged with quartz wool into a pear-shaped bottle. The filtrates were concentrated by a rotary evaporator under vacuum state and then dried by pure nitrogen. After reaction with 60 μL derivatization reagent (a mixture of 50 μL of N,O-bis-

171   (trimethylsilyl)trifluoroacetamide (BSTFA) and 1 % trimethylsilyl chloride and 10 μL

172   of pyridine) for 3 h at 70 °C in order to convert COOH and OH groups to the

173   corresponding trimethylsilyl esters and ethers. After cooling down to room

174   temperature, an aliquot of 40 μL internal standard (C_{13} n-alkene) was added into the

175   derivative solution prior to GC/MS analyses. All BSOA tracers were individually

176   identified by comparing mass spectra against authentic standards and literature data.

177   Whereas, due to the commercial unavailability of a subset of authentic standards, the

178   quantification of target compounds relied on the surrogate standards, expect for cis-

179   pinonic. Specifically, the erythritol was applied to determine the 2-methyltetrols, C_5-

180   alkene triols and 3-MeTHF-3,4-diols; The quantification of 2-methylglyceric acid, 3-

181   hydroxyglutaric acid, 3-methyl-1,2,3-butanetricarboxylic acid and β-caryophyllinic

182   acid was performed using glyceric acid, tartaric acid, suberic acid and cis-pinic acid,

183   respectively. This approach was also applied in other similar studies (Li et al., 2013;

184   Zhu et al., 2016). The standards solutions were spiked onto the blank filters to assess

185   to the recoveries, which ranged from 82% to 105%. Field blank filters were also

186   analyzed following the same analytical procedure as the ambient samples, with no

187   target compounds detected in these blanks.

188   Furthermore, partial filters were cut into pieces, and then extracted three times

189   under sonication with 15ml Milli-Q pure water (18.2 MΩ). Ten ions such as SO_4^{2-},

190   NO_3^-, Cl^-, NH_4^+, and K^+ were determined using ion chromatography (Dionex, ICS-

191   1100). A DRI model 2001 thermal–optical carbon analyzer was used to measure the

192   organic carbon (OC) and element carbon (EC) in each $PM_{2.5}$ filter samples, of which

water-soluble organic carbon (WSOC) was extracted into Mill-Q pure water (18.2

MΩ) and ultimately quantified by a total organic carbon (TOC) analyzer (Model

TOC-L CPH, Shimadzu, Japan).

2.3 Aerosol liquid water content (ALWC) and in situ pH

The thermodynamic model (ISORROPIA-II) can provide robust predictions of the

aerosol liquid water content (ALWC) and in situ pH in $PM_{2.5}$ samples. By combining

the actual temperature (T) and relative humidity (RH) in the atmosphere and the

composition, the ALWC and H^+ loads can be simulated, which are used for

calculating the situ pH.

2.4 Positive matrix factorization (PMF) source apportionment

As a receptor model, PMF is a mathematical approach to quantify the contribution

of sources to samples, and has been widely used in the source apportionment of air

pollutant. More details of model can be found on the EPA website

(https://www.epa.gov/air-research/epa-positive-matrix-factorization-50-fundamentals-

and-user-guide). In this work, the organic matter (OM), EC WSOC, secondary

inorganic ions, biogenic SOA of all the samples served as the fingerprint species to

identify potential sources of the BSOA at Mt. Hua. After extensive testing, the model

would output an optimal solution characterized by a minimal difference between Q_{True}

and Q_{Robust} and a $Q/Q_{expected}$ ratio approaching 1; This is indicative of the robust model

performance, as confirmed by the high correlation coefficients between input and

estimated values. Furthermore, as revealed in our pervious study (Wu et al., 2022), the

change of the main emission sources was insignificant in air mass lifting process on

Mt. Hua. Thus, the samples from both sites were added together as one data matrix.

Based on the Q values (Q_{True}: 2362.8 vs. Q_{Robust}: 2365.6; $Q/Q_{expected}$: 0.86) and interpretability, five factors were obtained as the optimal solution after numerous testes. And the model could commendably reconstruct the temporal profiles of the input species, showing significant correlations ($R^2 > 0.92$) between observed and simulated species.

2.5 Concentration-weighted trajectory (CWT) analysis

To identify the potential spatial sources of the high BSOA on Mt. Hua, a CWT analysis was conducted using the BSOA concentrations and air mass backward trajectories. The 12-hr backward trajectories at a height of 1100 m were calculated by Hybrid-Single Particle Lagrangian Integrated Trajectory (HYSPLIT) model on an hourly basis throughout the campaign. Due to the relatively low temporal resolution of filter samples, the averaged BSOA concentration was assigned to match all the trajectories corresponding to each sample. And the CWT analysis herein was subsequently performed using the Igor-based tool using the Igor-based tool (i.e., ZeFir v3.70); More details for the protocol can can be found in Petit et al. (2017). Briefly, a grid with 0.25° × 0.25° cell size was created to cover all the trajectories; Each grid cell would be assigned a weighted concentration, which obtained from the averaged BSOA concentration that have associated trajectories crossing the grid cell. A high value in a gird cell indicates that the air parcels passing through it were associated with high concentration at the receptor site.

3 Results and discussion

3.1 Overview of OM during the campaign

The bulk chemical compositions of PM$_{2.5}$ during the campaign have been reported in our previous work (Wu et al., 2022), and strongly substantiated that organic matter (OM) is the principal component of PM$_{2.5}$ at both surface and high-elevation sites, with a mass fraction of 32%~46%. For a deeper insight into the relative abundances, vertical variability and sources of OM among two sampling sites, a comprehensive comparison was presented in Figure 1. The OM concentration was 30±10 μg/m^3 at the surface, approximately three-fold of that aloft. Such abundant OM at surface was apparently driven by fresh emissions from nearby roads and residences, as evidenced by its strong correlation with hopanes (Figure S1(a), R^2=0.46, p<0.05) being a known tracer for combustion sources (Schauer et al., 1999); Whereas, a weak correlation between OM and hopanes was found at MF site, indicating the different sources for the OM aloft. Moreover, the surface OM was characterized by a higher nocturnal load, and exhibited a decreased trend before midafternoon (Figure S1(b)), which was thermally driven boundary layer growth. Nonetheless, an inverse diel pattern was observed at high elevation site with a daily OM peak at the moment (12:00~16:00) of strong photochemical activity (Figure S1(b)), suggesting that OM components aloft was probably driven by photochemistry.

To determine the sources of OM at both sites, we performed a positive matrix factorization (PMF) analysis, and identified five types of sources for OM (Figure S2). Among these sources, biomass burning (BB) and fossil fuel combustion were believed to be the primary sources for OM at the surface, accounting for 52% and ~18% of

OM (Figure 1c), respectively. This coincided with that in Xi'an (~ 43% for BB) and Lin Village (30%-40% for BB) located on Guanzhong plain (Elser et al., 2016; Li et al., 2022). Whereas, merely ~24% of OM was explained by above anthropogenic sources at MS site; and most of OM aloft was dominated by biogenic secondary organic aerosol (BSOA, Figure 1d), with a fractional contribution of ~43% being 7-fold of that for subaerial OM. This elucidated a significant influence of biogenic primary and secondary sources on OM aloft.

3.2 Abundance and spatiotemporal variations of BSOA tracers

To characterize the spatiotemporal variations of biogenic SOA among two sites, plenty of BSOA tracers including isoprene, monoterpene and sesquiterpene were quantified as summarized in Table1. The sum of detected BSOA tracers ranged 31 ng/m^3 to 459 ng/m^3 at MF site (269 ± 108 ng/m^3, Figure S3), which was slightly lower than that at MS site (277 ± 159 ng/m^3); Such spatial pattern was also observed at Mt. Tai on North China Plain (Yi et al., 2021), further underscoring the significance of biogenic sources in mountainous OM formation aloft. Specifically, isoprene SOA tracers (BSOA$_I$) as the dominant species accounted for ~70% of the identified BSOA tracers, with an average of 197 ± 127 ng/m^3 at MS site and 183 ± 81 ng/m^3 at MF site, respectively; These were comparable to that in the Kathmandu Valley of India (183 ± 81 ng/m^3) (Wan et al., 2019) and a mid-latitudinal forest zone (~240 ng/m^3) (Zhu et al., 2016), but ~2 orders of magnitude higher than those measured over the North Pacific (3.6 ng/m^3) (Fu et al., 2011). As for total monoterpene SOA tracers (BSOA$_M$) and sesquiterpene tracers (BSOA$_S$), their abundances were lower by a

factor of approximately 4~6 than $BSOA_I$, probably due to lower emissions of monoterpene and sesquiterpene from the vegetation in this region. Noteworthily, $BSOA_M$ exhibited a converse spatial pattern, with a high load at surface (MF: 52±23 ng/m^3 vs. MS: 32±20 ng/m^3). The coniferous plants, as primary emitter of monoterpene (Gagan et al., 2023), may be less densely distributed at the ground level relative to that on Mt. Hua; Thus, relatively abundant $BSOA_M$ at the surface is likely affect by intensive BB activities that can also release numerous monoterpenes, thereby potentially augmenting the surface $BSOA_M$ levels. This can be manifested by that $BSOA_M$ strongly correlated with levoglucosan being known as BB tracer, but weakly with C_{29}-alkane that mainly derived from vegetation emissions (Wang and Kawamura, 2005) (Figure S4).

3.2.1 Isoprene SOA tracers

A total of eight isoprene tracers formed by oxidated reactions of isoprene with NOx and OH_2· were identified in this study, namely C_5-alkene triols (cis-2-MTB, trans-2-MTB and 3-MTB), 2-MGA, 2-methyltetrols (2-MT and 2-ME) and 3-MeTHF-3,4-diols (trans-3-Methyltetrahydrofuran-3,4-diol and cis-3-Methyltetrahydrofuran-3,4-diol). The $BSOA_I$ at MF site exhibited a pronounced diurnal cycle, characterized by a higher daytime load with an afternoon peak of 210±96 ng/m^3 (Figure 2(a)). This pattern aligns with temperature-driven characteristic of isoprene emission (Pétron et al., 2001; Zeng et al., 2023). A positive correlation between $BSOA_I$ and temperature (R^2=0.63) implies that a substantial part of surface $BSOA_I$ was expected to be formed locally (Figure S5 (a)), given the short atmospheric lifetime of isoprene. Whereas,

BSOA$_I$ aloft was characterized by an inverse diurnal variation, with a moderate enhancement in the nocturnal load. As revealed by a high-elevation CWT analysis of BSOA$_I$ (Figure 3), relatively high nocturnal loading was distributed over Mt. Hua and adjacent regions, indicating that these SOA tracers aloft were significantly influenced by regional/super-regional transport, especially during the nighttime.

2-methyltetrols (2-MTLs), as the predominant species at both sites, were more abundant aloft (99 ± 69 ng/m^3) relative to surface site (74 ± 32 ng/m^3); The levels were comparable to the field measurements at Mt. Tai (98 ng/m^3) (Yi et al., 2021), Mt. Changbai (22~282 ng/m^3) (Wang et al., 2008) and in Mexico City (8~190 ng/m^3) (Cooke et al., 2024a). Recently, a forest observation demonstrated that 2-MTLs could be biologically produced and then directly emitted into the atmosphere (Ye et al., 2021). Whereas, there is no significant correlation between 2-MTLs and C$_{29}$-alkane mainly released by vegetation (Figure S4(b)), indicating that 2-MTLs at both sampling sites primarily derived from secondary formation rather than being directly emitted by vegetation. As the oxidation products of isoprene under low/free-NOx conditions, 2-MTLs at MF site were significantly formed during the daytime, and peaked at 12:00~16:00 LT (local time, 85 ng/m^3, Figure 2(b)), corresponding to the period of reduced NOx loads, high temperature and intense solar radiation. Conversely, the concentration of 2-MTLs aloft decreased progressively during the daytime, bottoming out at 16:00~20:00 LT; This inverse diurnal pattern was probably due to the influx of the surface NOx that was transported aloft by the prevailing valley breeze, which subsequently inhibited the 2-MTLs formation aloft. Meanwhile, such

325 relatively abundant NOx condition during the daytime would promote the formation

326 of 2-MGA aloft (culminating at 12:00~16:00 LT), as corroborated by a positive

327 correlation between 2-MGA and NO_2 (Figure S5 (c)). This finding was consistent with

328 the laboratory measurements of 2-MGA being derived from oxidization of isoprene

329 with high NOx load (Surratt et al., 2006; Szmigielski et al., 2007). Moreover, the

330 surface 2-MGA also exhibited a similar diurnal pattern with an average of 29±15

331 ng/m^3 being 1.8-fold of that aloft, albeit a weak relationship between 2-MGA and NO_2;

332 This appreciably suggested that, beyond NOx, other factors also drove the 2-MGA

333 formation at MF site.

334 C_5-alkene triols and 3-MeTHF-3,4-diols were another prevalent isoprene tracers, of

335 which concentrations were comparable among two sites (Table 1). As the

336 photooxidation products under low/free-NOx levels, above two tracers exhibited a

337 diurnal cycle paralleled to that of 2-MTLs at two sites, and were characterized by

338 higher loads during nighttime. Despite that, the correlation between C_5-alkene triols

339 and 3-MeTHF-3,4-diols (R^2>0.74) was more robust than that involving 2-MTLs. This

340 was probably owing to that C_5-alkene triols and 3-MeTHF-3,4-diols were mainly

341 formed via acid-catalyzed intermolecular rearrangement reactions of epoxy-diols (Lin

342 et al., 2012; Wang et al., 2005), whereas 2-MTLs are likely to the result from

343 nucleophilic addition of water to the ring opening of epoxy-diols (Surratt et al., 2010).

344 **3.2.2 Monoterpene SOA tracers**

345 The detected monoterpene tracers, including pinic acid (PA), cis-pinonic acid

346 (PNA), 3-hydroxyglutaric acid (3-HGA) and 3-methyl-1,2,3-butanetricarboxylic acid

(MBTCA), are mainly derived from photooxidation of α/β pinene initiated by ·OH and O_3; Therefore, those four tracers exhibited a similar diurnal pattern, peaking at 12:00~16:00 LT when ·OH and O_3 concentrations remained at highest daily level. Based on the chamber measurements, PA and PNA are the early-generation products of α/β pinene (Liu et al., 2022; Jaoui et al., 2005), merely accounting for ~10% and ~12%-17% of the $BSOA_M$, respectively. Strikingly, PNA at two sampling sites was more abundant by a factor of ~1.5 than PA, consistent with the observations at Mt. Tai, Mt. Huang and in Duke Forest, North Carolina (Wang et al., 2023; Bhat and Fraser, 2007; Yi et al., 2021). The saturation vapor pressure of PNA (~7.2×10^{-5} Pa at 298 K, estimated by the E-AIM model) is lower than that of PA (~2.0×10^{-4} Pa), thus, PNA can be readily nucleated and saturated in the atmosphere. Given that, PNA was expected to have a higher abundance in aerosol than PA.

During the campaign, MBTCA was the most abundant $BSOA_M$ tracer, explaining more than half of the surface $BSOA_M$ tracers at both sites, followed by 3-HGA with fractional contributions of ~20% to total $BSOA_M$. MBTCA and 3-HGA are regarded as the later-generation products of α/β-pinene, and can be derived from further photodegradation of PNA or PA; Thus, MBTCA/(PA+PNA) ratio (abbreviated as M/P hereafter) is commonly used to estimate the α/β-pinene-derived SOA aging, of which a higher value is indicative of more aged α/β-pinene SOA. As depicted in Figure S6, the M/P value (2.6±1.3) at MS site was ~1.4-fold of that at MF site, reflecting that the $BSOA_M$ tracers aloft were more aged compared to that at surface; This finding coincided with the variation of oxidation state of carbon (OSc) measured by the

aerosol mass spectrometer. Additionally, a clear diurnal pattern of M/P ratio was found at MF site, with a daily peak at 16:00~20:00 LT lagged that of MBTCA by ~4 hr. However, the diurnal cycle of the M/P ratio at MS site exhibited a bimodal pattern, with two nearly equivalent peaks during the daytime (16:00~20:00) and nighttime (4:00~8:00). Relatively high M/P ratios during nighttime indicated a more aged state of nocturnal α/β-pinene SOA at the upper atmosphere, markedly differing from the ground-based observations. This was partially due to that the nocturnal pollutants at MS site were mostly driven by regional or long-range transport (Figure 3), in which α/β-pinene SOA aloft would undergo a deeper aging, and leading to the high M/P ratio.

3.2.3 Sesquiterpene SOA tracers

As a typical and abundant sesquiterpene, β-caryophyllene has been widely studied due to its high reactivity and significant aerosol formation potential; and it can be oxidized into β-caryophyllinic acid via ozonolysis/photooxidation (Jaoui et al., 2007; Jaoui et al., 2003). In this study, β-caryophyllinic acid was found to exhibit a relatively high concentration among the detected BSOA tracers (Table 1), with an average of 35 ± 19 ng/m^3 at MF site and 56 ± 41 ng/m^3 at MS site, respectively; These loads were comparative to Mt. Wuyi (7.6-54 ng/m^3) (Ren et al., 2019) and Mt. Tai (0.05-48 ng/m^3) (Fu et al., 2012). As expected, β-caryophyllinic acid robustly correlated with the BSOA$_M$ ($R^2>0.60$, $p<0.05$) at both sampling sites, indicating similar formation pathways for these species. Additionally, the significant relationship between β-caryophyllinic acid and levoglucosan at MF site could be a result of

391 intensive biomass burning as indicated in section 3.1; This observation aligns with

392 previous findings that sesquiterpenes accumulated in leaves and wood can be released

393 in the biomass burning process, subsequently oxidized to form β-caryophyllinic acid

394 (Zhang et al., 2019b). Notably, β-caryophyllene SOA tracers aloft in this study

395 showed clearly enhanced concentrations during the daytime from 10:00 to 16:00;

396 whereas the diurnal cycle of β-caryophyllinic acid at MF site was less pronounced,

397 despite significant diurnal differences in O_3 load and temperature that are known to

398 influence heterogeneous reactions of β-caryophyllene.

3.3 Influencing factors of BSOA formation in upper troposphere

400   A comparison of diurnal cycles of mass fraction of BSOA to OM ($F_{BSOA/OM}$) among

401 both sampling sites is illustrated in Figure 4. At MF site, a spike in $F_{BSOA/OM}$ was

402 observed at around 12:00-16:00 (Figure 4(a)), demonstrating that the surface BSOA

403 formation was strongly enhanced in the presence of abundant O_3/OH radical load and

404 high biogenic emissions, especially for isoprene SOA; Such diurnal variation was in

405 good agreement with the measurements at other sites (Zhang et al., 2019b; Zhu et al.,

406 2016; Lee et al., 2016). Whereas $F_{BSOA/OM}$ for isoprene aloft exhibited a decreasing

407 pattern during the photochemically active period (Figure 4(b)), reaching a minimum

408 at 12:00-16:00 LT. Although oxidant levels remained relatively high at this time, the

409 $F_{BSOA/OM}$-isoprene was only 75% of that for the prior moment. Our previous

410 observational evidences have corroborated that surface anthropogenic pollutants can

411 be transported to the upper atmosphere by the prevailing valley breeze (Wu et al.,

412 2022; Wu et al., 2024). Those anthropogenic pollutants (e.g., SO_2, NOx) likely

413 modulated BSOA formation aloft, leading to above unusual diurnal cycle of $F_{BSOA/OM}$-

414 isoprene. To elucidate the above hypothesis, the mantel test and random forest (RF)

415 analysis were applied for daytime BSOA aloft. More descriptions and settings for the

416 models can be seen in the supplementary materials (Test S1).

3.3.1 Effects of meteorological factors on BSOA

418 As illustrated in Figure 5(a), the daytime $BSOA_I$ aloft positively correlated with

419 ambient temperature, consistent with the observations on Mt. Tai, Mt. Huang and Mt.

420 Wuyi (Ren et al., 2019; Wang et al., 2023; Yi et al., 2021). Given the temperature-

421 driven characteristic of isoprene emission (Pétron et al., 2001), relatively high

422 temperature was expected to enhance biogenic SOA yield through the photooxidation

423 of isoprene. While, $BSOA_M$ and $BSOA_S$ exhibited insignificantly negative

424 correlations with temperature (Figure 5(a)), indicating that their formation may be less

425 sensitive to temperature variations. Additionally, the strong temperature-dependence

426 of $BSOA_I$ also indicated a significant part of $BSOA_I$ tracers aloft undergo rapid in-situ

427 formation once the oxidants concentrations built up during the daytime, contrasting

428 with those during nighttime. An insignificant correlation was observed between

429 relative humidity and BSOA tracers ($|r|<0.08$, $P \geq 0.05$). However, the moist weather

430 frequently occurred at MS site, even during the daytime with average RH of 62 ± 19%

431 (Wu et al., 2022); Thus, the less pronounced variation can explain the insensitivity of

432 BSOA formation to RH. Even so, the high RH during the daytime could indirectly

433 influence BSOA formation aloft by modulating aerosol water content (ALWC),

434 aerosol acidity, gas–particle partitioning of BSOA precursors (Xu et al., 2015; Yan et

al., 2025; Isaacman-Vanwertz et al., 2016).

3.3.2 Effects of anthropogenic pollutants on BSOA

Evidence from laboratory studies referred to a nonlinear dependence of BSOA yield on NOx load, wherein the yield increases with rising NOx levels under low-NOx conditions, but exhibits a decreasing trend as NOx levels rise under high-NOx conditions (Xu et al., 2014; Xu et al., 2025). Whereas, the BSOA tracers aloft, especially isoprene-derived SOA, negatively correlated with NO_2 (r=0.36, P<0.05) (Figure 5(a)). Additionally, the 2-MTLs/2-MGA ratio, which is indicative of NOx influence on SOA formation, followed a similar diurnal pattern to that of the $F_{BSOA/OM}$-isoprene (Figure 5(b)). All those findings indicated that the NO_2 transported from the surface to high altitude may limit the formation of SOA_I in the daytime. As is well known, isoprene oxidization primarily follows two pathways, i.e., HO_2 pathway forming 2-MTLs in NOx-limited conditions and NO/NO_2 channel yielding 2-MGA in high-NOx scenarios (Surratt et al., 2010; Szmigielski et al., 2007). Thereby, we hypothesized that the increasing NOx at MS site may perturb BSOA formation by competing with the HO_2 pathway, diminishing the net SOA yield relative to NOx-limited conditions. This was consistent with experimental finding conducted by Thornton et al. (2020), who demonstrated that at a high NOx level (NO~500 ppt) that is akin to our daytime observations at MS site, the maximum BSOA yield is 10% lower than that at low NOx.

As shown in Figure 5(a), the sulfate presented a statistically significant positive relationship with $BSOA_I$. This feature appeared to be common for other similar field

studies (Wang et al., 2008; Xu et al., 2015; Liu et al., 2017), underscoring the significant role of sulfate in the isoprene-derived SOA formation. According to laboratory studies (Eddingsaas et al., 2010), the sulfate can act as nucleophiles to facilitate the ring-opening reaction of IEPOX, which is a pivotal oxidation product of isoprene when organic peroxy radicals mainly react with HO_2 radicals. While, the daytime sulfate level was moderately enhanced, peaking at 12:00-16:00 LT (Figure 5(c)); Additionally, a ~4% enhancement in the mass fraction of daytime sulfate was also observed at MS site compared to MF site (Figure S7(a)). These findings are indicative of the further formation in air mass lifting process (Wu et al., 2022). An increase in sulfate would boost the ionic strength and salting-in effect of aerosol, thereby enhancing IEPOX reactive uptake and inhibiting its reversible partitioning back to the gas phase. The SO_4^{2-}/HSO_4^- equilibrium is crucial for $BSOA_I$ yield under a highly acidic condition (Cooke et al., 2024b); While, the chemical form of inorganic S(VI) also shifts from HSO_4^- at MF site to SO_4^{2-} at MS site during vertical transport, which would facilitate $BSOA_I$ formation, as the nucleophilicity of SO_4^{2-} is two orders of magnitude higher than that of HSO_4^- (Aoki et al., 2020). As is well-known, sulfate can modulate the H^+ level, acting as a more efficient proton donor to catalyze IEPOX ring opening and isoprene ozonolysis; Thus, H^+ concentration predicted by the thermodynamic model ISORROPIA II positively correlates with $BSOA_I$ (r=0.37, P<0.05, Figure 5(a)). But a nonlinear relationship between the yields of methyltetrol sulfates/ 2-MTLs and under low pH (<3) condition is revealed in the chamber study (Cooke et al., 2024b); Based on our previous study (Wu et al., 2022), the average

daytime pH was 3.4±2.2 at MS site, indicating that there are other factors perturbing

BSOA formation at Mt. Hua, warranting further investigation.

Furthermore, the additional sulfate formation in lifting air mass can also promote

an enhancement in ALWC aloft, consistent with the strong positive correlation

observed between ALWC and sulfate (R^2=0.66, P<0.05, Figure S7). As demonstrated

in Figure 5(c), the daytime ALWC peaked at 12:00-16:00 LT, corresponding to a

significant decrease in $F_{BSOA-isoprene/OM}$. This pattern suggested an inhibited effect of

aerosol water on BSOA formation, consistent with laboratory observation by Gaston

et al. (2014), who found a 50% reduction in IEPOX reactive uptake on NH_4HSO_4

particles as RH increases from 30% to 70%. As evidenced by previous studies (Xu et

al., 2015; Riedel et al., 2015), the abundant aerosol water can moderate BSOA

formation by affecting ionic strength, proton donor/nucleophilic activity, and

consequently altering the reactive uptake (e.g., IEPOX) and subsequent reactions. To

quantitatively evaluate the effects of ALWC, the pseudo-first-order heterogeneous

reaction rate constant for IEPOX reactive uptake (k_{het}) was calculated for the samples

at MS site following the method of Gaston et al. (2014) (Text S2). The simulated

uptake coefficient of IEPOX (γ_{IEPOX}) during the daytime was 4.3×10^{-4}, being in the

range of field and laboratory observations ($0.1–6.5 \times 10^{-4}$) (Zhang et al., 2017; Gaston

et al., 2014). As shown in Figure 6, the high ALWC commonly corresponds to low

γ_{IEPOX} during the daytime, characterized by weak ionic strength and low $H^+_{(aq)}$

concentration. This indicates that enhanced ALWC at MS likely impeded the IEPOX

uptake onto particle surface. Consequently, the average k_{het} at 12:00-16:00 LT was

merely 9.8×10^{-8} 1/s, which was an order of magnitude lower than that in the rest of daytime. These results underscore that enhanced ALWC during the daytime would lead to an insufficiently rapid heterogeneous reaction of IEPOX, and finally diminished the $BSOA_I$ formation.

To elucidate the key factors that affect BSOA formation aloft, a random forest (RF) analysis was conducted for the daytime samples at MS site. The RF model commendably highlighted the significance of the factors contributing to $BSOA_I$ formation, as evidenced by the robust correlations between the predicted and observed data for both the training and testing datasets ($R^2 > 0.8$, Table S1), along with minimal error metrics. As shown in Figure 5(d), the daytime $BSOA_I$ concentration was largely affected by the ozone (~29%), with a robust positive correlation between them (Figure 5(a)); This indicated that enhanced O_3 is likely to augment isoprene oxidation products aloft. Additionally, NO_2 and ALWC also play pivotal roles in $BSOA_I$ formation, with the importance of ~19% and 13%, respectively; These findings further corroborated that the enhanced NOx may lead to an impedimental effect on the daytime BSOA formation in the upper boundary layer of Mt. Hua. Such limiting effect on isoprene-derived SOA formation under a high NOx scenario was also found in Eastern China and Amazon (Zhang et al., 2017; De Sa et al., 2017).

4 Summary and conclusion

The $PM_{2.5}$ samples with 4 h intervals were synchronously collected at mountain foot and mountainside of Mt. Hua, to elucidate the chemical evolution and spatiotemporal differences of the organic matter among two sites. At the MF site, the

anthropogenic emissions, such as biomass burning and fossil fuel combustion, were identified as substantial contributors to the OM, accounting for more than 70% of total OM. Whereas, only ~24% of OM aloft was derived from anthropogenic emissions, with biogenic secondary organic aerosol (43%) emerging as the predominant OM source aloft.

Three distinct types of BSOA tracers were identified, predominantly featuring isoprene-derived species. At MF site, most of the BSOA tracers were more abundant during the daytime and peaked at 12:00~16:00 LT, indicative of photochemical oxidation as the primary formation pathway. Whereas, there is a marked decrease in the absolute concentration and relative abundance of daytime isoprene-derived tracers in the upper atmosphere. This decline can be attributed to the intrusion of ground-level NOx, which significantly modifies $BSOA_I$ formation at higher altitudes by inhibiting the $HO_2\cdot$ oxidative pathway. Additionally, a further formation of sulfate in lifting air mass moderately enhanced ALWC aloft, leading to a low IEPOX reactive uptake on the particle surface, which would also limit the daytime $BSOA_I$ formation aloft. Unfortunately, our limited data does not allow us to peer into the fundamental mechanistic and kinetic details of this process. All these findings highlighted the complex and regional variability of the influences of NOx on BSOA formation. Over the past decade, atmospheric environment in China has undergone substantial changes due to unevenly implemented emission controls, resulting in much higher levels of NO_2 compared with SO_2 (Zheng et al., 2018). These alterations in pollutant emissions could substantially affect BSOA formation; Thus, there is an urgent need for long-

term characterization of BSOA to better assess its potential impacts on radiative

forcing, human health, and to fully understand the anthropogenic−biogenic

interactions.

Data availability. The data used in this study are freely available at

https://doi.org/10.5281/zenodo.15164940 (Wu, 2025). And Meteorological data and

hourly $PM_{2.5}$, NO_2, O_3 concentrations can be obtained from

https://doi.org/10.5281/zenodo.7413640 (Wu, 2022).

Author contributions. G.W. designed research and contributed analytic tools. C.W.,

C.C. and J.L. collected the samples. C.W. and Y.C. conducted the sample analysis.

C.W. and G.W. performed the data interpretation. C.W. wrote the paper. All authors

contributed to the paper with useful scientific discussions.

Competing interests. The authors declare no competing interest.

Acknowledgements. This work was financially supported by the National Natural

Science Foundation of China (grant no. 42477097, 42130704) and the National Key

Research and Development Program of China (grant no. 2023YFC3707401).

References

Aoki, E., Sarrimanolis, J. N., Lyon, S. A., and Elrod, M. J.: Determining the Relative Reactivity of Sulfate, Bisulfate, and Organosulfates with Epoxides on Secondary Organic Aerosol, Acs Earth and Space Chemistry, 4, 1793-1801, 10.1021/acsearthspacechem.0c00178, 2020.

Armstrong, N. C., Chen, Y., Cui, T., Zhang, Y., Christensen, C., Zhang, Z., Turpin, B. J., Chan, M. N., Gold, A., Ault, A. P., and Surratt, J. D.: Isoprene Epoxydiol-Derived Sulfated and Nonsulfated Oligomers Suppress Particulate Mass Loss during Oxidative Aging of Secondary Organic Aerosol, Environmental Science & Technology, 56, 10.1021/acs.est.2c03200, 2022.

Bhat, S. and Fraser, M. P.: Primary source attribution and analysis of α-pinene photooxidation products in Duke Forest, North Carolina, Atmospheric Environment, 41, 2958-2966, 10.1016/j.atmosenv.2006.12.018, 2007.

Coggon, M. M., Gkatzelis, G. I., McDonald, B. C., Gilman, J. B., Schwantes, R. H., Abuhassan, N., Aikin, K. C., Arend, M. F., Berkoff, T. A., Brown, S. S., Campos, T. L., Dickerson, R. R., Gronoff,

G., Hurley, J. F., Isaacman-VanWertz, G., Koss, A. R., Li, M., McKeen, S. A., Moshary, F., Peischl, J., Pospisilova, V., Ren, X., Wilson, A., Wu, Y., Trainer, M., and Warneke, C.: Volatile chemical product emissions enhance ozone and modulate urban chemistry, Proceedings of the National Academy of Sciences of the United States of America, 118, 10.1073/pnas.2026653118, 2021.

Cooke, M. E., Waters, C. M., Asare, J. Y., Mirrielees, J. A., Holen, A. L., Frauenheim, M. P., Zhang, Z., Gold, A., Pratt, K. A., Surratt, J. D., Ladino, L. A., and Ault, A. P.: Atmospheric Aerosol Sulfur Distribution and Speciation in Mexico City: Sulfate, Organosulfates, and Isoprene-Derived Secondary Organic Aerosol from Low NO Pathways, ACS ES&T Air, 1, 1037-1052, 10.1021/acsestair.4c00048, 2024a.

Cooke, M. E., Armstrong, N. C., Fankhauser, A. M., Chen, Y., Lei, Z., Zhang, Y., Ledsky, I. R., Turpin, B. J., Zhang, Z., Gold, A., McNeill, V. F., Surratt, J. D., and Ault, A. P.: Decreases in Epoxide-Driven Secondary Organic Aerosol Production under Highly Acidic Conditions: The Importance of Acid-Base Equilibria, Environmental Science & Technology, 58, 10675-10684, 10.1021/acs.est.3c10851, 2024b.

de Sa, S. S., Palm, B. B., Campuzano-Jost, P., Day, D. A., Newburn, M. K., Hu, W., Isaacman-VanWertz, G., Yee, L. D., Thalman, R., Brito, J., Carbone, S., Artaxo, P., Goldstein, A. H., Manzi, A. O., Souza, R. A. F., Mei, F., Shilling, J. E., Springston, S. R., Wang, J., Surratt, J. D., Alexander, M. L., Jimenez, J. L., and Martin, S. T.: Influence of urban pollution on the production of organic particulate matter from isoprene epoxydiols in central Amazonia, Atmospheric Chemistry and Physics, 17, 6611-6629, 10.5194/acp-17-6611-2017, 2017.

Dong, X., Liu, Y., Li, X., Yue, M., Liu, Y., Ma, Z., Zheng, H., Huang, R., and Wang, M.: Modeling Analysis of Biogenic Secondary Organic Aerosol Dependence on Anthropogenic Emissions in China, Environmental Science & Technology Letters, 9, 286-292, 10.1021/acs.estlett.2c00104, 2022.

Drozd, G. T., Woo, J. L., and McNeill, V. F.: Self-limited uptake of α-pinene oxide to acidic aerosol: the effects of liquid-liquid phase separation and implications for the formation of secondary organic aerosol and organosulfates from epoxides, Atmospheric Chemistry and Physics, 13, 8255-8263, 10.5194/acp-13-8255-2013, 2013.

Eddingsaas, N. C., VanderVelde, D. G., and Wennberg, P. O.: Kinetics and Products of the Acid-Catalyzed Ring-Opening of Atmospherically Relevant Butyl Epoxy Alcohols, Journal of Physical Chemistry A, 114, 8106-8113, 10.1021/jp103907c, 2010.

Elser, M., Huang, R.-J., Wolf, R., Slowik, J. G., Wang, Q., Canonaco, F., Li, G., Bozzetti, C., Daellenbach, K. R., Huang, Y., Zhang, R., Li, Z., Cao, J., Baltensperger, U., El-Haddad, I., and Prevot, A. S. H.: New insights into PM$_{2.5}$ chemical composition and sources in two major cities in China during extreme haze events using aerosol mass spectrometry, Atmospheric Chemistry and Physics, 16, 3207-3225, 10.5194/acp-16-3207-2016, 2016.

Fu, P., Kawamura, K., and Miura, K.: Molecular characterization of marine organic aerosols collected during a round-the-world cruise, Journal of Geophysical Research-Atmospheres, 116, 10.1029/2011jd015604, 2011.

Fu, P., Kawamura, K., Chen, J., and Miyazaki, Y.: Secondary Production of Organic Aerosols from Biogenic VOCs over Mt. Fuji, Japan, Environmental Science & Technology, 48, 8491-8497, 10.1021/es500794d, 2014.

Fu, P. Q., Kawamura, K., Chen, J., Li, J., Sun, Y. L., Liu, Y., Tachibana, E., Aggarwal, S. G., Okuzawa, K., Tanimoto, H., Kanaya, Y., and Wang, Z. F.: Diurnal variations of organic molecular tracers and

stable carbon isotopic composition in atmospheric aerosols over Mt. Tai in the North China Plain: an influence of biomass burning, Atmospheric Chemistry and Physics, 12, 8359-8375, 10.5194/acp-12-8359-2012, 2012.

Gagan, S., Sarang, K., Rudzinski, K. J., Liu, R., Szmigielski, R., and Zhang, Y.: Synthetic strategies for oxidation products from biogenic volatile organic compounds in the atmosphere: A review, Atmospheric Environment, 312, 10.1016/j.atmosenv.2023.120017, 2023.

Gaston, C. J., Riedel, T. P., Zhang, Z., Gold, A., Surratt, J. D., and Thornton, J. A.: Reactive Uptake of an Isoprene-Derived Epoxydiol to Submicron Aerosol Particles, Environmental Science & Technology, 48, 11178-11186, 10.1021/es5034266, 2014.

Guenther, A. B., Jiang, X., Heald, C. L., Sakulyanontvittaya, T., Duhl, T., Emmons, L. K., and Wang, X.: The Model of Emissions of Gases and Aerosols from Nature version 2.1 (MEGAN2.1): an extended and updated framework for modeling biogenic emissions, Geoscientific Model Development, 5, 1471-1492, 10.5194/gmd-5-1471-2012, 2012.

Hallquist, M., Wenger, J. C., Baltensperger, U., Rudich, Y., Simpson, D., Claeys, M., Dommen, J., Donahue, N. M., George, C., Goldstein, A. H., Hamilton, J. F., Herrmann, H., Hoffmann, T., Iinuma, Y., Jang, M., Jenkin, M. E., Jimenez, J. L., Kiendler-Scharr, A., Maenhaut, W., McFiggans, G., Mentel, T. F., Monod, A., Prevot, A. S. H., Seinfeld, J. H., Surratt, J. D., Szmigielski, R., and Wildt, J.: The formation, properties and impact of secondary organic aerosol: current and emerging issues, Atmospheric Chemistry and Physics, 9, 5155-5236, 10.5194/acp-9-5155-2009, 2009.

Hodnebrog, O., Myhre, G., and Samset, B. H.: How shorter black carbon lifetime alters its climate effect, Nature Communications, 5, 10.1038/ncomms6065, 2014.

Hodzic, A., Kasibhatla, P. S., Jo, D. S., Cappa, C. D., Jimenez, J. L., Madronich, S., and Park, R. J.: Rethinking the global secondary organic aerosol (SOA) budget: stronger production, faster removal, shorter lifetime, Atmospheric Chemistry and Physics, 16, 7917-7941, 10.5194/acp-16-7917-2016, 2016.

Isaacman-VanWertz, G., Yee, L. D., Kreisberg, N. M., Wernis, R., Moss, J. A., Hering, S. V., de Sa, S. S., Martin, S. T., Alexander, M. L., Palm, B. B., Hu, W., Campuzano-Jost, P., Day, D. A., Jimenez, J. L., Riva, M., Surratte, J. D., Viegas, J., Manzi, A., Edgerton, E., Baumann, K., Souza, R., Artaxo, P., and Goldstein, A. H.: Ambient Gas-Particle Partitioning of Tracers for Biogenic Oxidation, Environmental Science & Technology, 50, 9952-9962, 10.1021/acs.est.6b01674, 2016.

Jaoui, M., Leungsakul, S., and Kamens, R. M.: Gas and particle products distribution from the reaction of β-caryophyllene with ozone, Journal of Atmospheric Chemistry, 45, 261-287, 10.1023/a:1024263430285, 2003.

Jaoui, M., Kleindienst, T. E., Lewandowski, M., Offenberg, J. H., and Edney, E. O.: Identification and quantification of aerosol polar oxygenated compounds bearing carboxylic or hydroxyl groups. 2. Organic tracer compounds from monoterpenes, Environmental Science & Technology, 39, 5661-5673, 10.1021/es048111b, 2005.

Jaoui, M., Lewandowski, M., Kleindienst, T. E., Offenberg, J. H., and Edney, E. O.: β-caryophyllinic acid:: An atmospheric tracer for β-caryophyllene secondary organic aerosol, Geophysical Research Letters, 34, 10.1029/2006gl028827, 2007.

Kelly, J. M., Doherty, R. M., O'Connor, F. M., and Mann, G. W.: The impact of biogenic, anthropogenic, and biomass burning volatile organic compound emissions on regional and seasonal variations in secondary organic aerosol, Atmospheric Chemistry and Physics, 18, 7393-

662 7422, 10.5194/acp-18-7393-2018, 2018.

663 Kroll, J. H., Ng, N. L., Murphy, S. M., Flagan, R. C., and Seinfeld, J. H.: Secondary organic aerosol
664 formation from isoprene photooxidation, Environmental Science & Technology, 40, 1869-1877,
665 10.1021/es0524301, 2006.

666 Lee, A. K. Y., Abbatt, J. P. D., Leaitch, W. R., Li, S.-M., Sjostedt, S. J., Wentzell, J. J. B., Liggio, J., and
667 Macdonald, A. M.: Substantial secondary organic aerosol formation in a coniferous forest:
668 observations of both day- and nighttime chemistry, Atmospheric Chemistry and Physics, 16, 6721-
669 6733, 10.5194/acp-16-6721-2016, 2016.

670 Lei, Z., Chen, Y., Zhang, Y., Cooke, M. E., Ledsky, I. R., Armstrong, N. C., Olson, N. E., Zhang, Z.,
671 Gold, A., Surratt, J. D., and Ault, A. P.: Initial pH Governs Secondary Organic Aerosol Phase State
672 and Morphology after Uptake of Isoprene Epoxydiols (IEPDX), Environmental Science &
673 Technology, 56, 10596-10607, 10.1021/acs.est.2c01579, 2022.

674 Li, J., Li, J., Wang, G., Ho, K. F., Han, J., Dai, W., Wu, C., Cao, C., and Liu, L.: In-vitro oxidative
675 potential and inflammatory response of ambient PM$_{2.5}$ in a rural region of
676 Northwest China: Association with chemical compositions and source contribution,
677 Environmental Research, 205, 10.1016/j.envres.2021.112466, 2022.

678 Li, J. J., Wang, G. H., Cao, J. J., Wang, X. M., and Zhang, R. J.: Observation of biogenic secondary
679 organic aerosols in the atmosphere of a mountain site in central China: temperature and relative
680 humidity effects, Atmospheric Chemistry and Physics, 13, 11535-11549, 10.5194/acp-13-11535-
681 2013, 2013.

682 Lin, Y.-H., Zhang, Z., Docherty, K. S., Zhang, H., Budisulistiorini, S. H., Rubitschun, C. L., Shaw, S.
683 L., Knipping, E. M., Edgerton, E. S., Kleindienst, T. E., Gold, A., and Surratt, J. D.: Isoprene
684 Epoxydiols as Precursors to Secondary Organic Aerosol Formation: Acid-Catalyzed Reactive
685 Uptake Studies with Authentic Compounds, Environmental Science & Technology, 46, 250-258,
686 10.1021/es202554c, 2012.

687 Lin, Y.-H., Zhang, H., Pye, H. O. T., Zhang, Z., Marth, W. J., Park, S., Arashiro, M., Cui, T.,
688 Budisulistiorini, H., Sexton, K. G., Vizuete, W., Xie, Y., Luecken, D. J., Piletic, I. R., Edney, E. O.,
689 Bartolotti, L. J., Gold, A., and Surratt, J. D.: Epoxide as a precursor to secondary organic aerosol
690 formation from isoprene photooxidation in the presence of nitrogen oxides, Proceedings of the
691 National Academy of Sciences of the United States of America, 110, 6718-6723,
692 10.1073/pnas.1221150110, 2013.

693 Liu, J., Russell, L. M., Lee, A. K. Y., McKinney, K. A., Surratt, J. D., and Ziemann, P. J.: Observational
694 evidence for pollution-influenced selective uptake contributing to biogenic secondary organic
695 aerosols in the southeastern US, Geophysical Research Letters, 44, 8056-8064,
696 10.1002/2017gl074665, 2017.

697 Liu, J., D'Ambro, E. L., Lee, B. H., Schobesberger, S., Bell, D. M., Zaveri, R. A., Zelenyuk, A.,
698 Thornton, J. A., and Shilling, J. E.: Monoterpene Photooxidation in a Continuous-Flow Chamber:
699 SOA Yields and Impacts of Oxidants, NO$_x$, and VOC Precursors,
700 Environmental Science & Technology, 56, 12066-12076, 10.1021/acs.est.2c02630, 2022.

701 Marais, E. A., Jacob, D. J., Jimenez, J. L., Campuzano-Jost, P., Day, D. A., Hu, W., Krechmer, J., Zhu,
702 L., Kim, P. S., Miller, C. C., Fisher, J. A., Travis, K., Yu, K., Hanisco, T. F., Wolfe, G. M.,
703 Arkinson, H. L., Pye, H. O. T., Froyd, K. D., Liao, J., and McNeill, V. F.: Aqueous-phase
704 mechanism for secondary organic aerosol formation from isoprene: application to the southeast
705 United States and co-benefit of SO$_2$ emission controls, Atmospheric Chemistry and

Physics, 16, 1603-1618, 10.5194/acp-16-1603-2016, 2016.

McFiggans, G., Mentel, T. F., Wildt, J., Pullinen, I., Kang, S., Kleist, E., Schmitt, S., Springer, M., Tillmann, R., Wu, C., Zhao, D., Hallquist, M., Faxon, C., Le Breton, M., Hallquist, A. M., Simpson, D., Bergstrom, R., Jenkin, M. E., Ehn, M., Thornton, J. A., Alfarra, M. R., Bannan, T. J., Percival, C. J., Priestley, M., Topping, D., and Kiendler-Scharr, A.: Secondary organic aerosol reduced by mixture of atmospheric vapours, Nature, 565, 587-593, 10.1038/s41586-018-0871-y, 2019.

Mellouki, A., Wallington, T. J., and Chen, J.: Atmospheric Chemistry of Oxygenated Volatile Organic Compounds: Impacts on Air Quality and Climate, Chemical Reviews, 115, 3984-4014, 10.1021/cr500549n, 2015.

Nazarenko, L., Rind, D., Tsigaridis, K., Del Genio, A. D., Kelley, M., and Tausnev, N.: Interactive nature of climate change and aerosol forcing, Journal of Geophysical Research-Atmospheres, 122, 3457-3480, 10.1002/2016jd025809, 2017.

Ng, N. L., Brown, S. S., Archibald, A. T., Atlas, E., Cohen, R. C., Crowley, J. N., Day, D. A., Donahue, N. M., Fry, J. L., Fuchs, H., Griffin, R. J., Guzman, M. I., Herrmann, H., Hodzic, A., Iinuma, Y., Jimenez, J. L., Kiendler-Scharr, A., Lee, B. H., Luecken, D. J., Mao, J., McLaren, R., Mutzel, A., Osthoff, H. D., Ouyang, B., Picquet-Varrault, B., Platt, U., Pye, H. O. T., Rudich, Y., Schwantes, R. H., Shiraiwa, M., Stutz, J., Thornton, J. A., Tilgner, A., Williams, B. J., and Zaveri, R. A.: Nitrate radicals and biogenic volatile organic compounds: oxidation, mechanisms, and organic aerosol, Atmospheric Chemistry and Physics, 17, 2103-2162, 10.5194/acp-17-2103-2017, 2017.

Petit, J. E., Favez, O., Albinet, A., and Canonaco, F.: A user-friendly tool for comprehensive evaluation of the geographical origins of atmospheric pollution: Wind and trajectory analyses, Environmental Modelling & Software, 88, 183-187, 10.1016/j.envsoft.2016.11.022, 2017.

Pétron, G., Harley, P., Greenberg, J., and Guenther, A.: Seasonal temperature variations influence isoprene emission, Geophysical Research Letters, 28, 1707-1710, 10.1029/2000gl011583, 2001.

Pye, H. O. T., Chan, A. W. H., Barkley, M. P., and Seinfeld, J. H.: Global modeling of organic aerosol: the importance of reactive nitrogen (NO_x and NO_3), Atmospheric Chemistry and Physics, 10, 11261-11276, 10.5194/acp-10-11261-2010, 2010.

Ren, Y., Wang, G., Tao, J., Zhang, Z., Wu, C., Wang, J., Li, J., Wei, J., Li, H., and Meng, F.: Seasonal characteristics of biogenic secondary organic aerosols at Mt. Wuyi in Southeastern China: Influence of anthropogenic pollutants, Environmental Pollution, 252, 493-500, 10.1016/j.envpol.2019.05.077, 2019.

Ridley, D. A., Heald, C. L., Ridley, K. J., and Kroll, J. H.: Causes and consequences of decreasing atmospheric organic aerosol in the United States, Proceedings of the National Academy of Sciences of the United States of America, 115, 290-295, 10.1073/pnas.1700387115, 2018.

Riedel, T. P., Lin, Y.-H., Budisulistiorini, H., Gaston, C. J., Thornton, J. A., Zhang, Z., Vizuete, W., Gold, A., and Surrattt, J. D.: Heterogeneous Reactions of Isoprene-Derived Epoxides: Reaction Probabilities and Molar Secondary Organic Aerosol Yield Estimates, Environmental Science & Technology Letters, 2, 38-42, 10.1021/ez500406f, 2015.

Riva, M., Chen, Y., Zhang, Y., Lei, Z., Olson, N. E., Boyer, H. C., Narayan, S., Yee, L. D., Green, H. S., Cui, T., Zhang, Z., Baumann, K., Fort, M., Edgerton, E., Budisulistiorini, S. H., Rose, C. A., Ribeiro, I. O., L e Oliveira, R., dos Santos, E. O., Machado, C. M. D., Szopa, S., Zhao, Y., Alves, E. G., de Sa, S. S., Hu, W., Knipping, E. M., Shaw, S. L., Duvoisin Junior, S., de Souza, R. A. F., Palm, B. B., Jimenez, J.-L., Glasius, M., Goldstein, A. H., Pye, H. O. T., Gold, A., Turpin, B. J.,

Vizuete, W., Martin, S. T., Thornton, J. A., Dutcher, C. S., Ault, A. P., and Surratt, J. D.: Increasing Isoprene Epoxydiol-to-Inorganic Sulfate Aerosol Ratio Results in Extensive Conversion of Inorganic Sulfate to Organosulfur Forms: Implications for Aerosol Physicochemical Properties, Environmental Science & Technology, 53, 8682-8694, 10.1021/acs.est.9b01019, 2019.

Schauer, J. J., Kleeman, M. J., Cass, G. R., and Simoneit, B. R. T.: Measurement of emissions from air pollution sources.: 2.: C_1 through C_{30} organic compounds from medium duty diesel trucks, Environmental Science & Technology, 33, 1578-1587, 10.1021/es980081n, 1999.

Scott, C. E., Rap, A., Spracklen, D. V., Forster, P. M., Carslaw, K. S., Mann, G. W., Pringle, K. J., Kivekas, N., Kulmala, M., Lihavainen, H., and Tunved, P.: The direct and indirect radiative effects of biogenic secondary organic aerosol, Atmospheric Chemistry and Physics, 14, 447-470, 10.5194/acp-14-447-2014, 2014.

Shrivastava, M., Cappa, C. D., Fan, J., Goldstein, A. H., Guenther, A. B., Jimenez, J. L., Kuang, C., Laskin, A., Martin, S. T., Ng, N. L., Petaja, T., Pierce, J. R., Rasch, P. J., Roldin, P., Seinfeld, J. H., Shilling, J., Smith, J. N., Thornton, J. A., Volkamer, R., Wang, J., Worsnop, D. R., Zaveri, R. A., Zelenyuk, A., and Zhang, Q.: Recent advances in understanding secondary organic aerosol: Implications for global climate forcing, Reviews of Geophysics, 55, 509-559, 10.1002/2016rg000540, 2017.

Surratt, J. D., Chan, A. W. H., Eddingsaas, N. C., Chan, M., Loza, C. L., Kwan, A. J., Hersey, S. P., Flagan, R. C., Wennberg, P. O., and Seinfeld, J. H.: Reactive intermediates revealed in secondary organic aerosol formation from isoprene, Proceedings of the National Academy of Sciences of the United States of America, 107, 6640-6645, 10.1073/pnas.0911114107, 2010.

Surratt, J. D., Murphy, S. M., Kroll, J. H., Ng, a. L. N., Hildebrandt, L., Sorooshian, A., Szmigielski, R., Vermeylen, R., Maenhaut, W., Claeys, M., Flagan, R. C., and Seinfeld, J. H.: Chemical composition of secondary organic aerosol formed from the photooxidation of isoprene, Journal of Physical Chemistry A, 110, 9665-9690, 10.1021/jp061734m, 2006.

Szmigielski, R., Surratt, J. D., Vermeylen, R., Szmigielska, K., Kroll, J. H., Ng, N. L., Murphy, S. M., Sorooshian, A., Seinfeld, J. H., and Claeys, M.: Characterization of 2-methylglyceric acid oligomers in secondary organic aerosol formed from the photooxidation of isoprene using trimethylsilylation and gas chromatography/ion trap mass spectrometry, Journal of Mass Spectrometry, 42, 101-116, 10.1002/jms.1146, 2007.

Thornton, J. A., Shilling, J. E., Shrivastava, M., D'Ambro, E. L., Zawadowicz, M. A., and Liu, J.: A Near-Explicit Mechanistic Evaluation of Isoprene Photochemical Secondary Organic Aerosol Formation and Evolution: Simulations of Multiple Chamber Experiments with and without Added NO_x, Acs Earth and Space Chemistry, 4, 1161-1181, 10.1021/acsearthspacechem.0c00118, 2020.

Wan, X., Kang, S., Rupakheti, M., Zhang, Q., Tripathee, L., Guo, J., Chen, P., Rupakheti, D., Panday, A. K., Lawrence, M. G., Kawamura, K., and Cong, Z.: Molecular characterization of organic aerosols in the Kathmandu Valley, Nepal: insights into primary and secondary sources, Atmospheric Chemistry and Physics, 19, 2725-2747, 10.5194/acp-19-2725-2019, 2019.

Wang, G., Zhang, R., Gomez, M. E., Yang, L., Zamora, M. L., Hu, M., Lin, Y., Peng, J., Guo, S., Meng, J., Li, J., Cheng, C., Hu, T., Ren, Y., Wang, Y., Gao, J., Cao, J., An, Z., Zhou, W., Li, G., Wang, J., Tian, P., Marrero-Ortiz, W., Secrest, J., Du, Z., Zheng, J., Shang, D., Zeng, L., Shao, M., Wang, W., Huang, Y., Wang, Y., Zhu, Y., Li, Y., Hu, J., Pan, B., Cai, L., Cheng, Y., Ji, Y., Zhang, F., Rosenfeld,

D., Liss, P. S., Duce, R. A., Kolb, C. E., and Molina, M. J.: Persistent sulfate formation from London Fog to Chinese haze, Proceedings of the National Academy of Sciences of the United States of America, 113, 13630-13635, 10.1073/pnas.1616540113, 2016.

Wang, G. H. and Kawamura, K.: Molecular characteristics of urban organic aerosols from Nanjing: A case study of a mega-city in China, Environmental Science & Technology, 39, 7430-7438, 10.1021/es051055+, 2005.

Wang, G. H., Li, J. J., Cheng, C. L., Zhou, B. H., Xie, M. J., Hu, S. Y., Meng, J. J., Sun, T., Ren, Y. Q., Cao, J. J., Liu, S. X., Zhang, T., and Zhao, Z. Z.: Observation of atmospheric aerosols at Mt. Hua and Mt. Tai in central and east China during spring 2009-Part 2: Impact of dust storm on organic aerosol composition and size distribution, Atmospheric Chemistry and Physics, 12, 4065-4080, 10.5194/acp-12-4065-2012, 2012.

Wang, W., Kourtchev, I., Graham, B., Cafmeyer, J., Maenhaut, W., and Claeys, M.: Characterization of oxygenated derivatives of isoprene related to 2-methyltetrols in Amazonian aerosols using trimethylsilylation and gas chromatography/ion trap mass spectrometry, Rapid Communications in Mass Spectrometry, 19, 1343-1351, 10.1002/rcm.1940, 2005.

Wang, W., Wu, M. H., Li, L., Zhang, T., Liu, X. D., Feng, J. L., Li, H. J., Wang, Y. J., Sheng, G. Y., Claeys, M., and Fu, J. M.: Polar organic tracers in PM$_{2.5}$ aerosols from forests in eastern China, Atmospheric Chemistry and Physics, 8, 7507-7518, 10.5194/acp-8-7507-2008, 2008.

Wang, Y., Meng, J., Huang, T., Ma, J., Wang, Y., Zhang, X., Guo, Q., Yang, J., and Hou, Z.: Contrasting molecular characteristics and formation mechanisms of biogenic and anthropogenic secondary organic aerosols at the summit and foot of Mt. Huang, East China, Science of the Total Environment, 895, 10.1016/j.scitotenv.2023.165116, 2023.

Wu, C.: Synchronous observation of biogenic secondary organic aerosol at Mt. Hua, Zenodo [data set], https://doi.org/10.5281/zenodo.15164940, 2025.

Wu, C.: Synchronous observation of aerosol at Mt. Hua, Version 1, Zenodo [data set], https://doi.org/10.5281/zenodo.7413640, 2022.

Wu, C., Liu, X., Zhang, K., Zhang, S., Cao, C., Li, J., Li, R., Zhang, F., and Wang, G.: Measurement report: Formation of tropospheric brown carbon in a lifting air mass, Atmospheric Chemistry and Physics, 24, 9263-9275, 10.5194/acp-24-9263-2024, 2024.

Wu, C., Cao, C., Li, J., Lv, S., Li, J., Liu, X., Zhang, S., Liu, S., Zhang, F., Meng, J., and Wang, G.: Different physicochemical behaviors of nitrate and ammonium duringtransport: a case study on Mt. Hua, China, Atmospheric Chemistry and Physics, 22, 15621-15635, 10.5194/acp-22-15621-2022, 2022.

Wu, K., Yang, X., Chen, D., Gu, S., Lu, Y., Jiang, Q., Wang, K., Ou, Y., Qian, Y., Shao, P., and Lu, S.: Estimation of biogenic VOC emissions and their corresponding impact on ozone and secondary organic aerosol formation in China, Atmospheric Research, 231, 10.1016/j.atmosres.2019.104656, 2020.

Xu, L., Kollman, M. S., Song, C., Shilling, J. E., and Ng, N. L.: Effects of NO_x on the Volatility of Secondary Organic Aerosol from Isoprene Photooxidation, Environmental Science & Technology, 48, 2253-2262, 10.1021/es404842g, 2014.

Xu, L., Middlebrook, A. M., Liao, J., de Gouw, J. A., Guo, H., Weber, R. J., Nenes, A., Lopez-Hilfiker, F. D., Lee, B. H., Thornton, J. A., Brock, C. A., Neuman, J. A., Nowak, J. B., Pollack, I. B., Welti, A., Graus, M., Warneke, C., and Ng, N. L.: Enhanced formation of isoprene-derived organic

838 aerosol in sulfur-rich power plant plumes during Southeast Nexus, Journal of Geophysical
839 Research-Atmospheres, 121, 11137-11153, 10.1002/2016jd025156, 2016.

840 Xu, L., Guo, H., Boyd, C. M., Klein, M., Bougiatioti, A., Cerully, K. M., Hite, J. R., Isaacman-
841 VanWertz, G., Kreisberg, N. M., Knote, C., Olson, K., Koss, A., Goldstein, A. H., Hering, S. V., de
842 Gouw, J., Baumann, K., Lee, S.-H., Nenes, A., Weber, R. J., and Ng, N. L.: Effects of
843 anthropogenic emissions on aerosol formation from isoprene and monoterpenes in the
844 southeastern United States, Proceedings of the National Academy of Sciences of the United States
845 of America, 112, 37-42, 10.1073/pnas.1417609112, 2015.

846 Xu, X., Wang, G., Gao, Y., Zhang, S., Chen, L., Li, R., Li, Z., and Li, R.: Smog chamber study on the
847 NOx dependence of SOA from isoprene photo-oxidation: implication on RO2 chemistry, Journal
848 of Environmental Sciences, https://doi.org/10.1016/j.jes.2025.05.024, 2025.

849 Yan, J., Armstrong, N. C., Kolozsvari, K. R., Waters, C. M., Xiao, Y., Fankhauser, A. M., Cooke, M. E.,
850 Frauenheim, M., Buchenau, N. A., Parham, R. L., Zhang, Z., Turpin, B. J., Lambe, A. T., Gold, A.,
851 Ault, A. P., and Surratt, J. D.: Effect of Initial Seed Aerosol Acidity on the Kinetics and Products
852 of Heterogeneous Hydroxyl Radical Oxidation of Isoprene Epoxydiol-Derived Secondary Organic
853 Aerosol, Journal of Physical Chemistry A, 129, 4132-4147, 10.1021/acs.jpca.4c08082, 2025.

854 Ye, J., Batista, C. E., Guimaraes, P. C., Ribeiro, I. O., Vidoudez, C., Barbosa, R. G., Oliveira, R. L., Ma,
855 Y., Jardine, K. J., Surratt, J. D., Guenther, A. B., Souza, R. A. F., and Martin, S. T.: Near-canopy
856 horizontal concentration heterogeneity of semivolatile oxygenated organic compounds and
857 implications for 2-methyltetrols primary emissions, Environmental Science-Atmospheres, 1, 8-20,
858 10.1039/d0ea00006j, 2021.

859 Yi, Y., Meng, J., Hou, Z., Wang, G., Zhou, R., Li, Z., Li, Y., Chen, M., Liu, X., Li, H., and Yan, L.:
860 Contrasting compositions and sources of organic aerosol markers in summertime $PM_{2.5}$
861 from urban and mountainous regions in the North China Plain, Science of the Total
862 Environment, 766, 10.1016/j.scitotenv.2020.144187, 2021.

863 Zeng, J., Zhang, Y., Mu, Z., Pang, W., Zhang, H., Wu, Z., Song, W., and Wang, X.: Temperature and
864 light dependency of isoprene and monoterpene emissions from tropical and subtropical trees:
865 Field observations in south China, Applied Geochemistry, 155, 10.1016/j.apgeochem.2023.105727,
866 2023.

867 Zhang, H., Yee, L. D., Lee, B. H., Curtis, M. P., Worton, D. R., Isaacman-VanWertz, G., Offenberg, J.
868 H., Lewandowski, M., Kleindienst, T. E., Beaver, M. R., Holder, A. L., Lonneman, W. A.,
869 Docherty, K. S., Jaoui, M., Pye, H. O. T., Hu, W., Day, D. A., Campuzano-Jost, P., Jimenez, J. L.,
870 Guo, H., Weber, R. J., de Gouw, J., Koss, A. R., Edgerton, E. S., Brune, W., Mohr, C., Lopez-
871 Hilfiker, F. D., Lutz, A., Kreisberg, N. M., Spielman, S. R., Hering, S. V., Wilson, K. R., Thornton,
872 J. A., and Goldstein, A. H.: Monoterpenes are the largest source of summertime organic aerosol in
873 the southeastern United States, Proceedings of the National Academy of Sciences of the United
874 States of America, 115, 2038-2043, 10.1073/pnas.1717513115, 2018a.

875 Zhang, Q., Zheng, Y., Tong, D., Shao, M., Wang, S., Zhang, Y., Xu, X., Wang, J., He, H., Liu, W., Ding,
876 Y., Lei, Y., Li, J., Wang, Z., Zhang, X., Wang, Y., Cheng, J., Liu, Y., Shi, Q., Yan, L., Geng, G.,
877 Hong, C., Li, M., Liu, F., Zheng, B., Cao, J., Ding, A., Gao, J., Fu, Q., Huo, J., Liu, B., Liu, Z.,
878 Yang, F., He, K., and Hao, J.: Drivers of improved $PM_{2.5}$ air quality in China from
879 2013 to 2017, Proceedings of the National Academy of Sciences of the United States of America,
880 116, 24463-24469, 10.1073/pnas.1907956116, 2019a.

881 Zhang, Y.-Q., Chen, D.-H., Ding, X., Li, J., Zhang, T., Wang, J.-Q., Cheng, Q., Jiang, H., Song, W., Ou,

882   Y.-B., Ye, P.-L., Zhang, G., and Wang, X.-M.: Impact of anthropogenic emissions on biogenic
883   secondary organic aerosol: observation in the Pearl River Delta, southern China, Atmospheric
884   Chemistry and Physics, 19, 14403-14415, 10.5194/acp-19-14403-2019, 2019b.

885 Zhang, Y., Tang, L., Sun, Y., Favez, O., Canonaco, F., Albinet, A., Couvidat, F., Liu, D., Jayne, J. T.,
886   Wang, Z., Croteau, P. L., Canagaratna, M. R., Zhou, H.-c., Prevot, A. S. H., and Worsnop, D. R.:
887   Limited formation of isoprene epoxydiols-derived secondary organic aerosol under NOx-rich
888   environments in Eastern China, Geophysical Research Letters, 44, 2035-2043,
889   10.1002/2016gl072368, 2017.

890 Zhang, Y., Chen, Y., Lambe, A. T., Olson, N. E., Lei, Z., Craig, R. L., Zhang, Z., Gold, A., Onasch, T.
891   B., Jayne, J. T., Worsnop, D. R., Gaston, C. J., Thornton, J. A., Vizuete, W., Ault, A. P., and Surratt,
892   J. D.: Effect of the Aerosol-Phase State on Secondary Organic Aerosol Formation from the
893   Reactive Uptake of Isoprene-Derived Epoxydiols (IEPDX), Environmental Science & Technology
894   Letters, 5, 167-174, 10.1021/acs.estlett.8b00044, 2018b.

895 Zheng, B., Tong, D., Li, M., Liu, F., Hong, C., Geng, G., Li, H., Li, X., Peng, L., Qi, J., Yan, L., Zhang,
896   Y., Zhao, H., Zheng, Y., He, K., and Zhang, Q.: Trends in China's anthropogenic emissions since
897   2010 as the consequence of clean air actions, Atmospheric Chemistry and Physics, 18, 14095-
898   14111, 10.5194/acp-18-14095-2018, 2018.

899 Zheng, Y., Horowitz, L. W. W., Menzel, R., Paynter, D. J., Naik, V., Li, J., and Mao, J.: Anthropogenic
900   amplification of biogenic secondary organic aerosol production, Atmospheric Chemistry and
901   Physics, 23, 8993-9007, 10.5194/acp-23-8993-2023, 2023.

902 Zhu, C., Kawamura, K., Fukuda, Y., Mochida, M., and Iwamoto, Y.: Fungal spores overwhelm biogenic
903   organic aerosols in a midlatitudinal forest, Atmospheric Chemistry and Physics, 16, 7497-7506,
904   10.5194/acp-16-7497-2016, 2016.

905

906

907

908

909 **Table 1** Summary of the average BSOA tracers at the two sampling sites during the
910 whole campaign.

Compounds	Mountain foot			Mountainside		
	Average	Daytime	nighttime	Average	Daytime	nighttime
Isoprene derived SOA tracers						
2-MGA[a]	29±15	36±17	22±7	16±8	20±9	13±6
2-methyltetrols						
2-Methylthreitol	24±10	25±10	23±10	32±23	29±21	36±24
2-Methylerythritol	50±2	52±23	48±21	67±46	57±42	76±49
subtotal	74±32	77±33	71±31	99±68	86±62	112±72
C$_5$-alkene triols						
cis-2-Me-1,3,4-THB[b]	20±13	20±13	20±13	22±18	19±15	24±20
3-Me-2,3,4-THB[c]	23±15	22±14	23±16	23±19	21±17	26±21
trans-2-Me-1,3,4-THB[d]	31±19	30±19	31±19	30±22	26±19	33±25
subtotal	74±46	73±45	74±48	75±59	66±51	83±66
3-MeTHF-3,4-diols						
trans-3-Me-THF-diol[e]	3±1	3±1	3±1	3±2	3±2	3±2
cis-3-Me-THF-diol[f]	4±2	4±2	4±2	4.7±3.7	4±3	5±4
subtotal	7±3	7±3	7±3	8±6	8±5	8±6
Total	182±81	191±83	173±77	197±126	178±114	216±135
α/β-pinene derived SOA tracers						
cis-pinonic acid	9±4	9±4	9±4	4±2	4±2	4±3
pinic acid	5±2	6±2	5±2	3±2	4±2	3±2
MBTCA[g]	26±14	30±14	23±14	19±13	21±14	18±12
3-HGA[h]	12±6	14±6	11±6	6±4	7±5	4±3
Total	52±23	59±22	46±22	32±20	36±21	28±18
β-caryophyllene derived SOA tracer						
β-Caryophyllinic acid	35±19	35±17	34±20	56±40	70±46	42±28

911 [a]2-MGA: 2-methylglyceric acid;

912 [b]cis-2-Me-1,3,4-THB: cis-2-Methyl-1,3,4-trihydroxy-1-butene;

913 [c]3-Me-2,3,4-THB: 3-Methyl-2,3,4-trihydroxy-1-butene;

914 [d]trans-2-Me-1,3,4-THB: trans-2-Methyl-1,3,4-trihydroxy-1-butene;

915 [e]trans-3-Me-TH-diol: trans-3-Methyltetrahydrofuran-3,4-diol;

916 [f]cis-3-Me-TH-diol: cis-3-Methyltetrahydrofuran-3,4-diol;

917 [g]MBTCA: 3-methyl-1,2,3-butanetricarboxylic acid;

918 [h]3-HGA: 3-Hydorxyglutaric acid

919
920
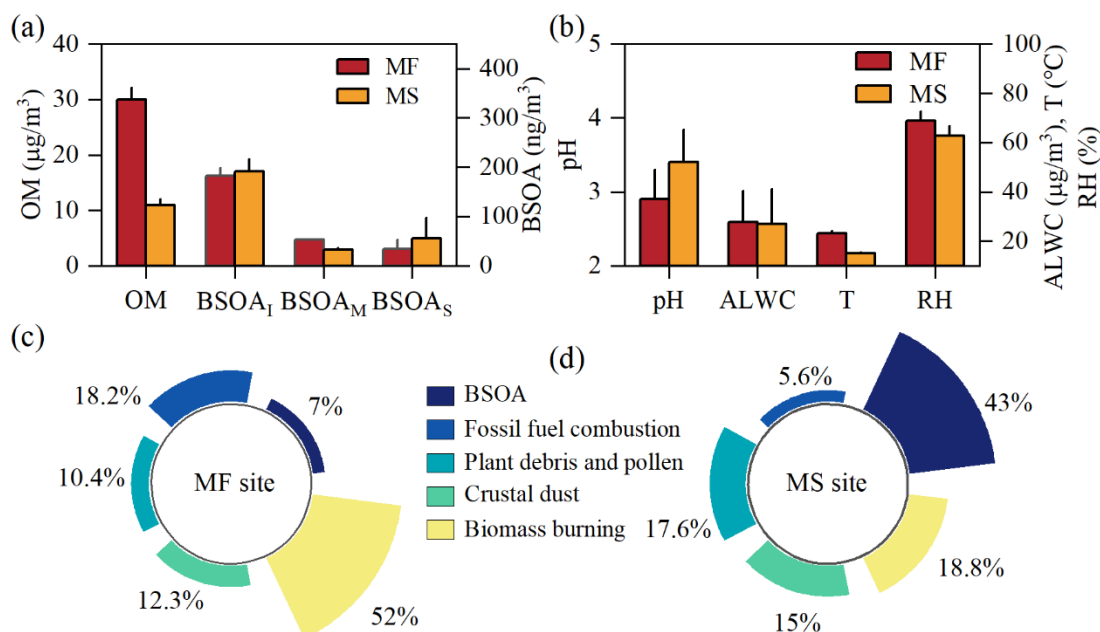
921
922 **Figure 1** Comparisons upon chemical composition **(a)**, meteorological conditions **(b)**,
923 and sources for OM **(c and d)** among two sampling sites. (OM concentration is
924 converted by the OM/OC ratio measured in our previous (Wu et al., 2024))

925
926
927

928
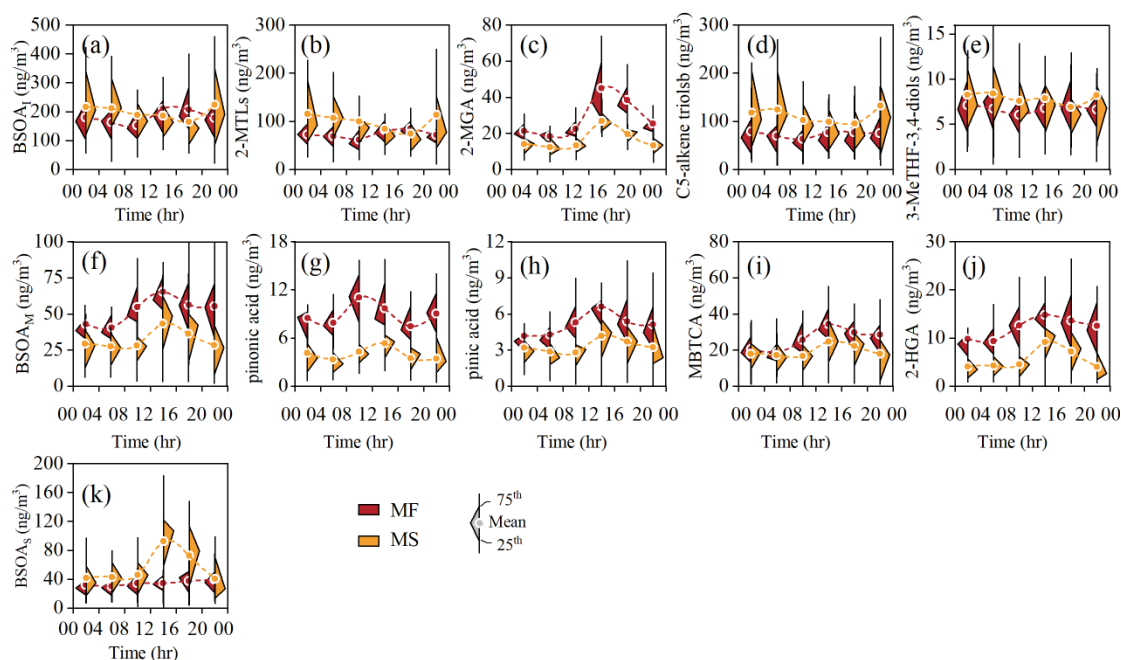
929 **Figure 2** Diurnal variations in BOSA tracers among both sites. **(a-e)** isoprene-derived
930 SOA tracer; **(f-j)** monoterpenes-derived SOA tracer; **(k)** β-caryophyllene -derived
931 SOA tracer.
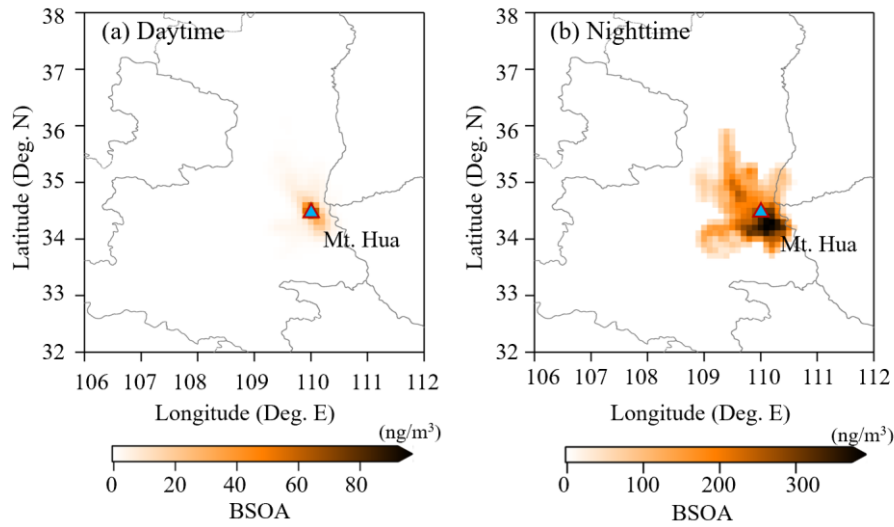
Figure 3 A concentration-weighted trajectory (CWT) analysis for $BSOA_I$ at MS site.
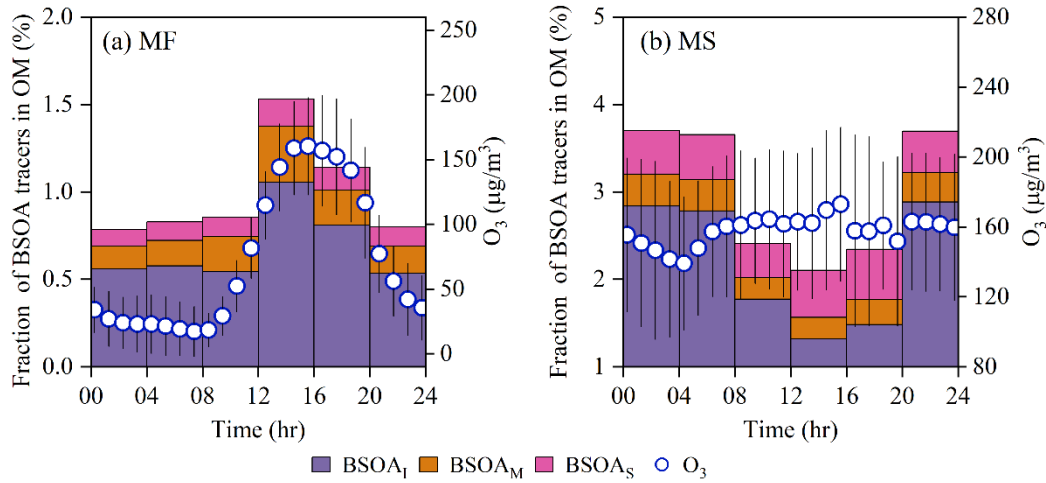
Figure 4 Diurnal cycles of mass fraction of BSOA tracers in OM and O_3 at both sampling sites.

943
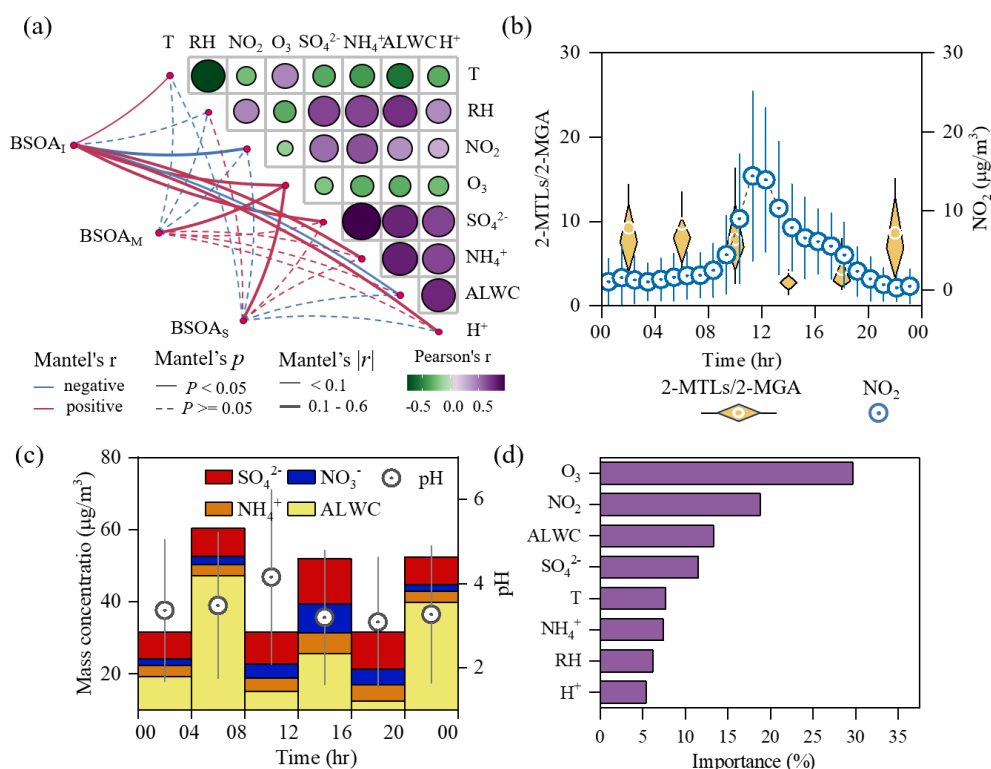
944 **Figure 5** Formation of daytime isoprene-derived SOA in upper troposphere. **(a)**
945 Mantel test between BSOA tracers and potential influencing factors at MS site; **(b**
946 **and c)** Diurnal variations 2-MTLs/2-MGA ratio, pH, and the concentration of NO_2,
947 SNA, ALWC at MS site; **(d)** Importance assessment for the key factors affecting the
948 daytime isoprene-derived SOA at the MS site.

949

950

951

952
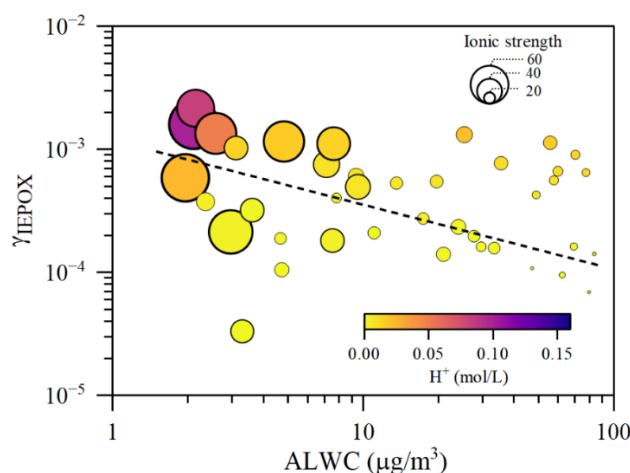
953 **Figure 6** Reactive uptake (γ_{IEPOX}) as a function of ALWC during the daytime at MS
954 site.